Oxygen Separation through U-Shaped Hollow Fiber Membrane Using Pure CO_2 as Sweep Gas

Yanying Wei, Jun Tang, Lingyi Zhou, Jian Xue, Zhong Li, and Haihui Wang
School of Chemistry and Chemical Engineering, South China University of Technology, 510640 Guangzhou, China

DOI 10.1002/aic.12802
Published online November 28, 2011 in Wiley Online Library (wileyonlinelibrary.com).

A number of U-shaped K_2NiF_4-type oxide hollow fiber membranes based on $(Pr_{0.9}La_{0.1})_2(Ni_{0.74}Cu_{0.21}Ga_{0.05})O_{4+\delta}$ (PLNCG) were successfully prepared by a phase inversion spinning process. The PLNCG hollow fiber membranes were then used to investigate the effect of CO_2 concentration in both the sweep gas and the feed air on the oxygen permeation flux. With pure CO_2 as the sweep gas and even 10% CO_2 in the feed air, a steady oxygen permeation flux of 0.9 mL/min·cm^2 (STP) is obtained at 975°C during 310 h, and no decline of the oxygen permeation flux is observed. XRD, SEM and EDS characterizations show the spent membrane still maintains the intact microstructure and perfect K_2NiF_4-type phase structure without carbonate, which indicates that the U-shaped PLNCG hollow fiber membrane is a very stable membrane under CO_2 atmosphere and has great potential for the practical application in oxyfuel techniques for CO_2 capture and storage. © 2011 American Institute of Chemical Engineers *AIChE J,* 58: 2856–2864, 2012
Keywords: hollow fiber, membrane, oxygen permeation, CO_2, mixed conductor

Introduction

The atmospheric CO_2 concentration has steadily increased from 280 ppm to its current value of 385 ppm since the industrial revolution, representing an increase of 35%.[1–3] It is mainly due to the unabated emission of CO_2 from the consumption of fossil fuels such as coal, oil and natural gas. Around the world, coal combustion is responsible for 42% of the CO_2 emission as providing 41% of the electricity.[4] Therefore, CO_2 capture and storage technologies (CCS) used to reduce the CO_2 emission from coal-fired power plants have gained increasing attentions. Currently, there are mainly three methods for CO_2 sequestration: precombustion separation, postcombustion capture and oxyfuel combustion techniques.[5–7] Recently, mixed conducting ceramic membranes with oxygen ionic and electronic conductivity have attracted increasing attentions due to their potential applications in oxygen supplying for power stations with CO_2 sequestration according to the oxyfuel concept.[8–13] In the oxyfuel process, oxygen diluted with recycled CO_2 is used to burn fossil fuels, resulting in a flue gas mainly consisted of CO_2 and H_2O which can be separated easily with condensation. For this reason, the mixed conducting oxygen permeable membrane used in oxyfuel process should not only have good oxygen permeability, but also good stability especially under atmosphere with high concentration of CO_2.

Most studies of mixed conducting oxygen permeable membrane have been concentrated on the perovskite-type oxides which have relatively high-oxygen permeation fluxes.[14–25] Unfortunately, most of the perovskite material are quite sensitive to CO_2. The membranes containing alkaline-earth elements such as Ba and Sr tend to react with acidic gas CO_2 to form carbonates.[26–36] Several groups[26–32] found that the oxygen permeation fluxes through the perovskite membranes containing alkaline-earth elements had a serious decrease due to the formation of carbonate layer even when a very low concentration of CO_2 was added to the sweep gas. It was also found that CO_2 in the feed air has a significant effect on the oxygen permeation fluxes[32–34] through the perovskite membranes containing alkaline-earth elements such as $BaCo_{0.4}Fe_{0.4}Zr_{0.2}O_{3-\delta}$, $Sr_{0.95}Co_{0.8}Fe_{0.2}O_{3-\delta}$ and $Ba_{0.5}Sr_{0.5}Co_{0.8}Fe_{0.2}O_{3-\delta}$ (BSCF) membranes. Jin et al.[35,36] also found the lifetime of perovskite membrane reactor which coupled the thermal decomposition of CO_2 with the POM reaction was not more than 40 h.

Therefore, intensive efforts have been made to develop the CO_2-tolerant mixed conduting oxides. It is reported that the stabiliy in the CO_2-containing atmosphere can be improved by proper doping such as Zr-doped $BaCe_{0.8}Y_{0.2}O_{3-\delta}$ (BCY)[37] and Ti-doped $SrCo_{0.8}Fe_{0.2}O_{3-\delta}$.[38] On the other hand, A-site-deficient perovskite oxides, such as $La_{0.2}Sr_{0.8}Co_{0.41}Fe_{0.41}Cu_{0.21}O_{3-\delta}$[39] and $La_{0.85}Ce_{0.1}Ga_{0.3}Fe_{0.65}Al_{0.05}O_{3-\delta}$[40] were also found to possess an enhanced resistance against the corrosion of CO_2. Recently, Luo et al.[41] developed a novel cobalt-free dual phase CO_2-tolerated oxygen permeable membrane. However, most of those aforementioned material were just tested in a low CO_2 concentration atomosphere, and the oxygen permeation fluxes decreased significantly once pure CO_2 was used as the sweep gas.

In the power plant concept with CO_2 sequestration, a part of the effluent gas is used as sweep gas, i.e., the sweep gas for the oxygen separator is consisted of about 80 vol % CO_2. This concept requires CO_2 resistant membranes without Ba and Sr, like doped La-Ni oxides.[42,43] Recently,

Correspondence concerning this article should be addressed to H. Wang at hhwang@scut.edu.cn.

Table 1. Preparation Conditions for the U-shaped PLNCG Hollow Fiber Membranes

Parameter	Value
Compositions of the starting solution	
PLNCG powder	52.60 wt%
PESf, A-300	9.29 wt%
NMP	37.18 wt%
PVP, K30	0.93 wt%
Spinning temperature	25°C
Injection rate of internal coagulant	2.8 ml/min
Spinning pressure	0.05 bar
Air gap	0.5 cm
Sintering temperature	1300 °C
Sintering time	3 h
Air flow rate for sintering	60 ml/min

Yashima et al.[44] investigated the oxygen permeability, electrical properties and detailed crystal structure of K_2NiF_4-type $(Pr_{0.9}La_{0.1})_2(Ni_{0.74}Cu_{0.21}Ga_{0.05})O_{4+\delta}$ (PLNCG). It can be expected that the PLNCG should exhibit good resistance to CO_2 because it is alkaline-earth elements free membrane. In our previous work, we found that this material has a good stability in CO_2-containing atomosphere. In this work, the PLNCG hollow fiber membranes are prepared by phase inversion/sintering technology,[45–52] the oxygen permeability and stability under pure CO_2 atomosphere on the sweep side while high oncentration of CO_2 on the feed air are investigated in detail. According to our previous work,[53] the U-shaped hollow fiber membrane can avoid the breakage of the membrane due to the expansion or shrinkage at varying temperatures. Therefore, the U-shaped PLNCG hollow fiber membranes are chosen in this study.

Experimental

The sol–gel route based on citric acid and EDTA as complexing and gelation agents has been adapted to prepare the PLNCG powder. To summarize, Ga was dissolved in nitric acid first, and proper amounts of $Pr(NO_3)_3{\cdot}6H_2O$, $La(NO_3)_3{\cdot}6H_2O$, $Ni(CH_3COO)_2{\cdot}4H_2O$, $Cu(NO_3)_2{\cdot}3H_2O$ were dissolved in water followed by the addition of citric acid, EDTA and $NH_3{\cdot}H_2O$. The mixture was then evaporated at 150°C under constant stirring to obtain a dark-green gel. Afterward, the gel was ignited to flame to get the precursor. The precursor was ground and calcined at temperatures up to 950°C for 10 h with a heating rate of 2°C/min to remove the residual carbon and form the desired K_2NiF_4-type structure. For spinning hollow fiber membranes, the powder was ball-milled for 24 h and then was dried using a spray dryer (Büchi mini spray dryer, B-290) with a nozzle of 1 μm. The obtained fine powder was used for the preparation of the U-shaped hollow fiber membrane.

The U-shaped PLNCG hollow fibers were fabricated using a wet spinning/sintering technology.[53] The spinning solution was composed of 9.29 wt% poly(ether sulfone) (PESf, A-300, BASF), 37.18 wt % 1-Methyl-2-pyrrolidinone (NMP, AR Grade, purity > 99.8%, Kermel Chem, Inc., Tianjin, China), 0.93 wt % polyvinyl pyrrolidone (PVP, K30, Boao biotech co, Shanghai, China) and 52.60 wt % PLNCG powder. A spinneret with an orifice diameter and inner diameter of 1.5 and 1.0 mm, respectively, was used to obtain the hollow-fiber precursors. Deionized water and tap water were used as the internal and external coagulants, respectively. Afterwards, the PLNCG hollow fiber precursors were sintered at 1300°C for 3 h with the air flow rate of 60 mL/min to remove the polymer and get gas-tight membrane. The preparation conditions are summarized in Table 1.

The phase structure of the as-prepared PLNCG powder, the fresh hollow fiber membrane after sintering at 1300°C and the spent hollow fiber membrane was characterized by X-ray diffraction (XRD, Bruker-D8 ADVANCE, Cu Kα radiation). The microstructure and morphology of the fresh and spent PLNCG hollow fiber were observed by a scanning electron microscope (SEM, JEOL JSM-6490LA). The oxygen permeation fluxes through the U-shaped PLNCG hollow fiber membranes under CO_2-containing atomosphere were investigated in a high-temperature permeation cell, as shown in Figure 1. The effective membrane area in this experiment is 1.2 cm^2. The U-shaped PLNCG hollow fiber membrane was sealed in a corundum tube with two channels by a commercial ceramic sealant (HT767, Hutian, China) as shown in Figure 2B. Air or a mixture of CO_2, O_2 and N_2 was fed to the shell side while He or CO_2 or a mixture of He and CO_2 swept on the core side to collect the permeated oxygen through the membrane. Helium is used for comparison in order to check how CO_2 is going to affect the flux. The gas-flow rates were controlled by mass-flow controllers (MFC, Seven Star D08-4F/ZM) calibrated using a soap bubble flow meter. The composition of the permeated gases were measured using an online gas chromatograph (GC, Agilent 7890) with a TCD detector. The leakage of the oxygen due to the imperfect sealing at high temperatures was less than 0.5% during all the experiments. Assuming that the leakage of nitrogen and oxygen through pores or cracks is in accordance with Knudsen diffusion, the fluxes of leaked N_2 and O_2 are related by

$$K = J_{N_2}^{\text{Leak}} : J_{O_2}^{\text{Leak}} = \sqrt{32/28} \times \frac{C_{N_2}^{\text{feed}}}{C_{O_2}^{\text{feed}}}. \quad (1)$$

The O_2 permeation flux was then calculated as follows

$$J_{O_2}(\text{ml}/\text{min}\cdot\text{cm}^2) = [C_{O_2}^{\text{core}} - \frac{C_{N_2}^{\text{core}}}{K}]\frac{F}{S} \quad (2)$$

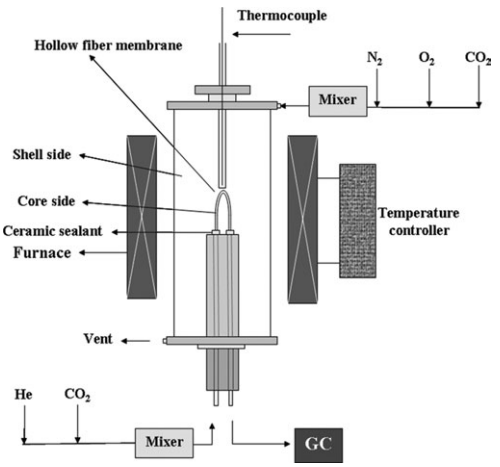

Figure 1. Oxygen permeation apparatus for the U-shaped PLNCG hollow fiber membrane at high temperature.

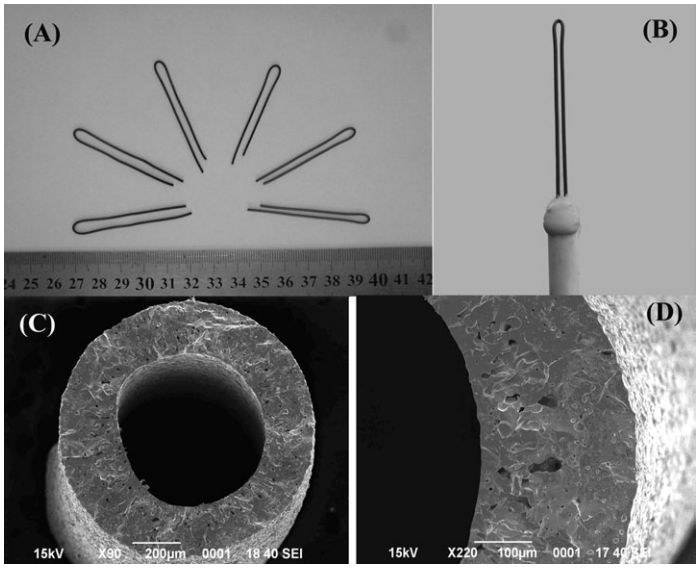

Figure 2. Photos and SEM micrographs of the U-shaped PLNCG hollow fiber membrane.

(A) photos of sintered hollow fiber membrane, (B) hollow fiber membrane fixed on the reactor, (C) SEM micrographs of cross section, and (D) the wall of the hollow fiber membrane.

Where $C_{O_2}^{\text{feed}}$, $C_{N_2}^{\text{feed}}$ are the oxygen concentration and nitrogen concentration on the shell side, which are adjusted by mass-flow controllers $C_{O_2}^{\text{core}}$, $C_{N_2}^{\text{core}}$ are the oxygen concentration and nitrogen concentration on the core side, which are calculated from the GC measurements. F is the flow rate of the exhaust stream, which can be measured by the soap flow meter, and S is the hollow fiber membrane effective area.

Results and Discussion

Figure 2A shows the photoof U-shaped PLNCG hollow fiber membranes after sintering at 1300°C for 3 h. The SEM micrographs of the cross section, and the wall of the sintered hollow fiber membrane are also shown in Figure 2C and D. The finger-like structures can be observed in the micrographs of PLNCG hollow fiber membranes.

The effects of CO_2 concentration in the sweep gas and the feed air, the flow rate of pure CO_2 (as the sweep gas) on the oxygen permeation flux through the U-shaped PLNCG hollow fiber membrane are investigated at different temperatures. The reversibility and stability of oxygen permeation flux under air/CO_2 gradient are also been studied this work.

Figure 3 presents the effects of CO_2 concentration in the sweep gas on the oxygen permeation fluxes through the U-shaped PLNCG hollow fiber membrane at different temperatures. The flow rate of sweep gas was 60 mL/min (STP) on the core side. It can be seen from Figure 3 that the oxygen permeation flux increases with increasing temperature because both of the oxygen surface exchange and bulk diffusion are improved at high temperatures. When CO_2 is introduced into the sweep gas, the oxygen permeation fluxes only decrease slightly. The oxygen permeation flux through the PLNCG hollow fiber membrane only decreases from 0.98 mL/min.cm^2 (STP) under Air/He gradient to 0.92 mL/min·cm^2 (STP) under Air/CO_2 gradient when the sweep gas flow rate is 60 mL/min (STP) at 975°C. In other words, when the pure CO_2 is used as the sweep gas instead of pure He, only 6.1% decrease of oxygen permeation flux is observed at a flow rate of 60 mL/min (STP) on the core side. The decrease of oxygen permeation flux when switching the sweep gas from He to CO_2 is due to the adsorption of CO_2 on the membrane surface, and decreases the oxygen exchange rate. The effect is more noticeable at low temperature. A decrease around 7.7% of the oxygen permeation flux is observed when temperature decreases from 975 to 950°C. Similar results were also found by other researchers.[41] It also can be observed in Figure 3B that the oxygen permeation fluxes through the PLNCG hollow fiber membrane only slightly change with varying concentration of CO_2 on the core side at differernt temperatures.

Figure 4 shows the dependence of the oxygen permeation flux on the flow rate of sweep CO_2 at different temperatures. Obviously, even when the pure CO_2 is used as the sweep gas, the oxygen permeation fluxes increase with the increasing sweep CO_2 flow rates. This is attributed to the higher flow rate sweep gas dilutes the permeated oxygen concentration and lowers the oxygen partial pressure on the core side, which leads to a higher oxygen permeation driving force. Moreover, the oxygen permeation flux is more sensitive to the effect of CO_2 flow rate at high temperatures. When the CO_2 flow rate was increased from 15 to 60 mL/min (STP), the oxygen permeation fluxes increases from 0.65 to 0.92 mL/min·cm^2 (STP) and 0.14 to 0.17 mL/min·cm^2 (STP) at 975 and 850°C, respectively. It also can be noted from Figure 4B that the gaps of corresponding permeated oxygen permeation fluxes under different CO_2 flow rate at high temperatures are bigger than that at low temperatures, i.e., the oxygen permeation flux is more sensitive to the effect of the CO_2 flow rate on the core side at high temperatures than that at low temperatures. In fact, it is unpraticed using such a big sweep gas flow to get oxygen in practice. For the oxyfuel combustion based on the oxygen permeable membrane, the required sweep gas flow is related to the effective membrane area and the oxygen permeation flux, which can make the oxygen concentration higher than 20%, i.e., the fossil fuels can combust in an oxygen-enriched air compared with the ordinary air. In the corresponding Arrhenius plot (shown in

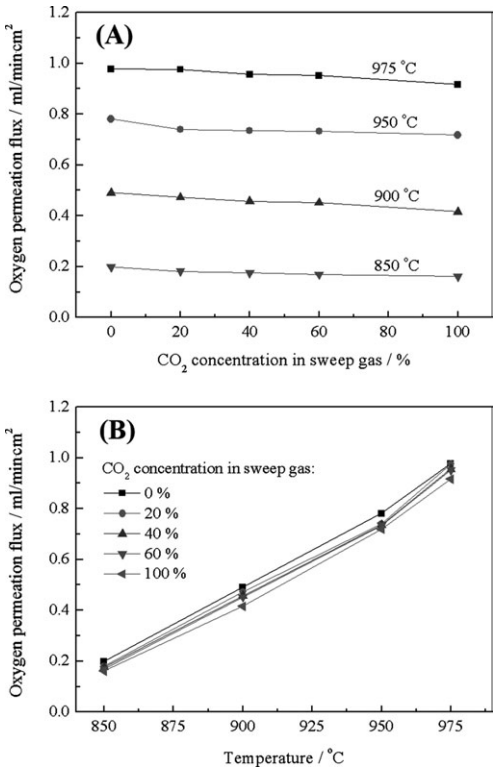

Figure 3. Effects of CO_2 concentration in the sweep gas on the oxygen permeation fluxes through the U-shaped PLNCG hollow fiber membrane at different temperatures.

Conditions: F_{air} = 180 mL/min, F_{sweep} = 60 mL/min.

Figure 5), a straight line is found which gives an apparent activation energy of 69.75 kJ/mol for the U-shaped PLNCG hollow fiber membrane at the temperature range of 850–975°C when the pure CO_2 is used as the sweep gas.

Figure 6 shows the reversibility of the oxygen permeation flux through the PLNCG hollow fiber membrane while periodically changing the sweep gas between pure He and pure CO_2 at 975°C. When He is used as the sweep gas, the oxygen permeation flux of 0.95 mL/min·cm^2 (STP) is obtained. When the sweep gas is changed from He to CO_2, the oxygen permeation flux is reduced to 0.90 mL/min·cm^2 (STP). Only a slight decrease of the oxygen permeation flux through the PLNCG hollow fiber membrane is observed. For the $Ba_{0.5}Sr_{0.5}Co_{0.8}Fe_{0.2}O_{3-\delta}$ (BSCF) perovskite membrane, the oxygen permeation flux stopped immediately when pure CO_2 was used as sweep gas at 875°C.[26] On the other hand, when the sweep gas is shifted back to pure He, the oxygen permeation flux through the PLNCG hollow fiber membrane can be recovered immediately. During the two cycles of the sweep gas shifting between He and CO_2, the oxygen permeation flux through the PLNCG hollow fiber membrane exhibits good CO_2-resistance and excellent reversibility.

As previously presented, the oxygen permeation flux through the PLNCG membrane is not significantly reduced when the pure CO_2 was used as the sweep gas, which indicates that the PLNCG possesses high-oxygen permeation flux and good stability under pure CO_2. However, some researchers found that when CO_2 was introduced into the feed air, the oxygen permeation flux through some CO_2-sensitive membrane had a sharp decrease as well.[32–34]

Therefore, the effects of CO_2 concentration in the feed air on the oxygen permeation fluxes through the U-shaped PLNCG hollow fiber membrane at different temperatures is investigated here. In this experiment, the oxygen partial pressure on the shell side keeps 0.21 atm, and the CO_2 concentration is controlled by adjusting the ratio of N_2 and CO_2. As shown in Figure 7, when the concentration of CO_2 in the feed air increases from 0 to 60%, the oxygen permeation flux maintains the initial oxygen permeation flux at temperatures from 850 to 950°C. Only at a higher temperature, such as 975°C, a slight decrease of the oxygen permeation flux is observed. The oxygen permeation flux through the PLNCG hollow fiber membrane changes from 0.94 mL/min·cm^2 (STP) to 0.93 mL/min·cm^2 (STP) when the CO_2 concentration in the feed air increases from 0 to 10% CO_2 at 975°C. Afterward, with the increase of CO_2 content in the feed air, the oxygen permeation fluxes are almost constant, which indicates PLNCG is really a kind of CO_2-stable meterail. It can also be found in Figure 7B that the oxygen permeation fluxes through the PLNCG hollow fiber membrane maintain a constant value with varying CO_2 concentration in the feed air at each temperature. However, Park et al.[34] found the oxygen permeation flux through BSCF disk membrane dereased from 1.4 to 0.8 mL/min·cm^2 when 700 ppm (0.07%) CO_2 was introduced into the feed air at 950°C, nearly 43% decrease of oxygen permeation flux was observed. Tong et al.[32] also found the oxygen permeation flux through $BaCo_{0.4}Fe_{0.4}Zr_{0.2}O_{3-\delta}$ disk membrane dereased from 0.88 to 0.79 mL/min·cm^2 when 10% CO_2 was introduced into the feed air at 950°C. Compared to these material, the effect of

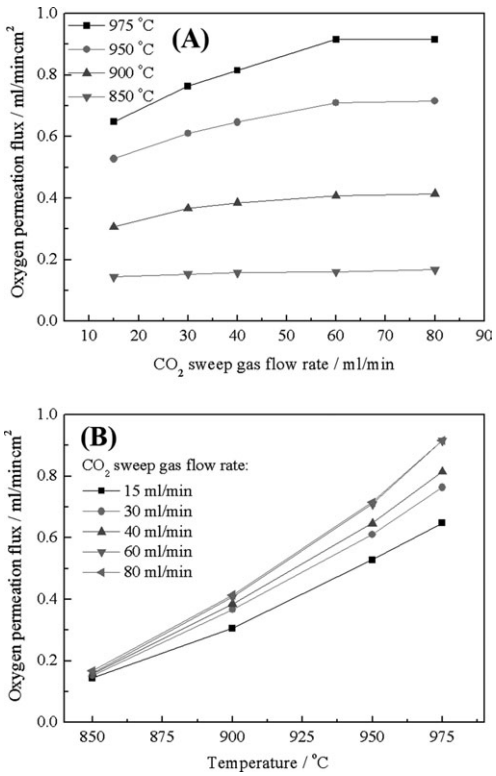

Figure 4. Effects of the flow rate of pure CO_2 as the sweep gas on the oxygen permeation fluxes through the U-shaped PLNCG hollow fiber membrane at different temperatures.

Conditions: F_{air} = 180 mL/min, Cco_2 = 100%.

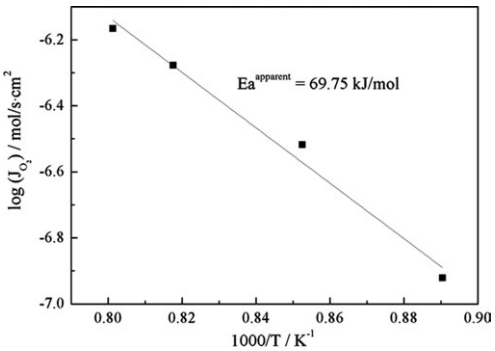

Figure 5. Arrhenius plot of the oxygen permeation flux of the U-shaped PLNCG hollow fiber membrane at the temperature range of 850–975°C when the pure CO_2 is used as the sweep gas.

CO_2 in the feed air on the oxygen permeation flux through PLNCG hollow fiber membrane is negligible and PLNCG exhibits a good stability under CO_2 atomsphere.

Figure 8 presents the oxygen permeation fluxes through the U-shaped PLNCG and BSCF hollow fiber membranes with different CO_2 concentration in the sweep gas on the core side. As known, BSCF is a good membrane but chemically less stable among many perovskite materials.[21] The oxygen permeation flux through the U-shaped BSCF hollow fiber membrane at 950°C is above 4.0 mL/min·cm^2 (STP) under air/He gradient. However, the oxygen permeation flux through the BSCF hollow fiber membrane sharply drops to 1.4 mL/min·cm^2 (STP) when 20% CO_2 is added to the sweep gas. Furthermore, it decreases gradually with time when a mixture of 20% CO_2 and 80% He was used as the sweep gas. After 2 h' operation, the oxygen permeation flux declines to 1.0 mL/min·cm^2 (STP), which is only 25% of the initial oxygen permeation flux when using pure He as the sweep gas. When the CO_2 concentration in the sweep gas increases to 40%, the oxygen permeation flux through the BSCF hollow fiber membrane declines to only 0.2 mL/min·cm^2 (STP). An immediate stop of the oxygen permeation flux through the BSCF hollow fiber membrane is observed when pure CO_2 is used as the sweep gas, which has also been found in the disk membrane by Arnold et al.[26] It is known that the alkaline-earth metal ions of Ba and Sr on the A site of perovskite structure are sensitive to CO_2 and tend to react with CO_2 to form carbonate, which leads to the decrease of oxygen permeation flux. Compared with BSCF, the oxygen permeation flux through the U-shaped PLNCG hollow fiber membrane is much stable under different CO_2 concentrations (from 0 to 100%) in the sweep gas on the core side. Although the oxygen permeation flux through the PLNCG hollow fiber membrane is not as high as that through BSCF hollow fiber membrane when pure He is used as the sweep gas, it keeps the initial oxygen permeation flux of aournd 1.0 mL/min·cm^2 (STP) all the time even when the pure CO_2 was used as the sweep gas. The results domentrate that PLNCG shows much better CO_2-tolerable property than the perovskite containing alkaline-earth metal. The possible reason is that there is no alkaline-earth metal element in such a K_2NiF_4-type material.

Figure 9A shows the oxygen permeation flux as a function of time through the PLNCG hollow fiber membrane using pure CO_2 as the sweep gas at 975°C. During this oxygen permeation test, a steady oxygen permeation flux of about 0.9 mL/min·cm^2 (STP) is obtained at 975°C with the CO_2 sweep-flow rate of 60 mL/min (STP), and the oxygen concentration of the down stream kept around 1.8 kPa. The oxygen permeation flux keeps constant even after 310 h and no decrease is observed. Many literatures have reported that the oxygen permeation fluxes through oxygen permeable membranes decreased sharply when the CO_2 was introduced into either the sweep gas[26–32] or the feed air.[32–34] It was found that the oxygen permeation flux through BSCF membranes decreases rapidly once CO_2 gas is introduced into the sweep side.[26] It was also noted that when CO_2 was added in the feed air on the shell side, the oxygen permeation fluxes through $BaCo_{0.4}Fe_{0.4}Zr_{0.2}O_{3-\delta}$, $Sr_{0.95}Co_{0.8}Fe_{0.2}O_{3-\delta}$ and BSCF membranes decreased due to the instability of these membranes in CO_2-containing atomsphere.[32–34] Therefore, it can be presumed that the oxygen permeation flux will have a rather bigger decrease if CO_2 exists in both the sweep gas and the feed air. In order to examine the stability of the PLNCG hollow fiber membrane in a more rigorous condition, the oxygen permeation flux through the PLNCG membrane is investigated when both the sweep gas and the feed air contains CO_2, as shown in Figure 9B. In this experiment, the pure CO_2 with the flow rate of 60 mL/min (STP) is used as the sweep gas on the core side, while 4 and 10% CO_2 is introduced into the feed air, respectively. As shown in Figure 9A, during the 310 h oxygen permeation test, the oxygen permeation flux keeps constant even though CO_2 exsists simultaneously on the both sides of the hollow fiber membrane, which indicates the good stability of PLNCG under CO_2-containing atomosphere. Compared with these CO_2-sensitive material mentioned previously, PLNCG exhibits excellent CO_2 tolerance.

After the 310 h' oxygen permeation test through the U-shaped PLNCG hollow fiber membrane at 975°C, the sample is characterized by XRD, SEM and EDS. Figure 10 presents the phase structures of the PLNCG powder prepared by a combined EDTA-citrate complexation, the fresh hollow fiber membrane sintered at 1300°C and the spent hollow fiber membrane after 310 h' oxygen permeation with pure CO_2 as the sweep gas and CO_2-containing air as the feed gas (Figure 9). The X-ray diffraction patterns indicate all of them are pure K_2NiF_4-structure. Furthermore, after the 310

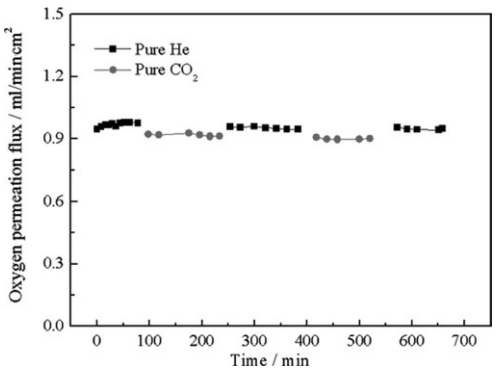

Figure 6. Reversibility of the oxygen permeation flux through the U-shaped PLNCG hollow fiber membrane while changing the sweep gas between pure He and pure CO_2.

Conditions: T = 975°C, F_{air} = 180 mL/min, F_{He}=F_{CO_2} = 60 mL/min.

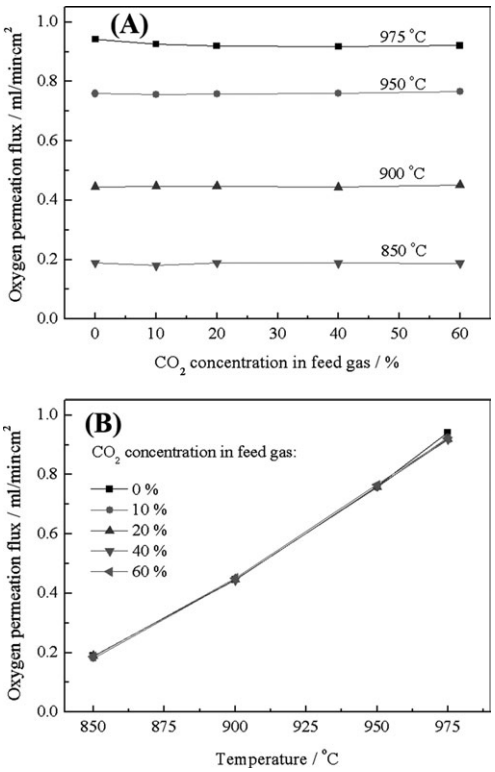

Figure 7. Effects of CO_2 concentration in the feed air on the oxygen permeation fluxes through the U-shaped PLNCG hollow fiber membrane at different temperatures.

Conditions: $F_{N_2+\ O2+CO2} = 150$ mL/min, $F_{He} = 60$ mL/min.

h' oxygen permeation operation, no carbonate is observed which indicates that the U-shaped PLNCG hollow fiber membrane exhibits excellent phase structure stability under CO_2 atomspheres.

Figure 11 also shows the SEM micrographs of the fresh and spent PLNCG hollow fiber membrane after 310 h' permeation test in CO_2 containing atomosphere. Figure 11A and B shows the inner and outer surface of the fresh PLNCG

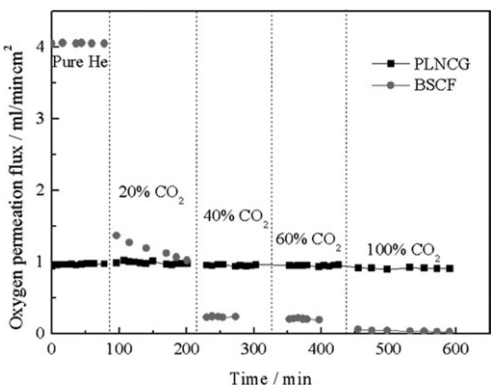

Figure 8. Oxygen permeation fluxes through the U-shaped BSCF and PLNCG hollow fiber membrane with different CO_2 concentration in the sweep gas.

Conditions: CO_2 concentration in the sweep gas varied from 0 to 100;% BSCF: $T = 950$°C, $F_{air} = 150$ mL/min, $F_{sweep} = 100$ mL/min; PLNCG: $T = 975$°C, $F_{air} = 180$ mL/min, $F_{sweep} = 60$ mL/min.

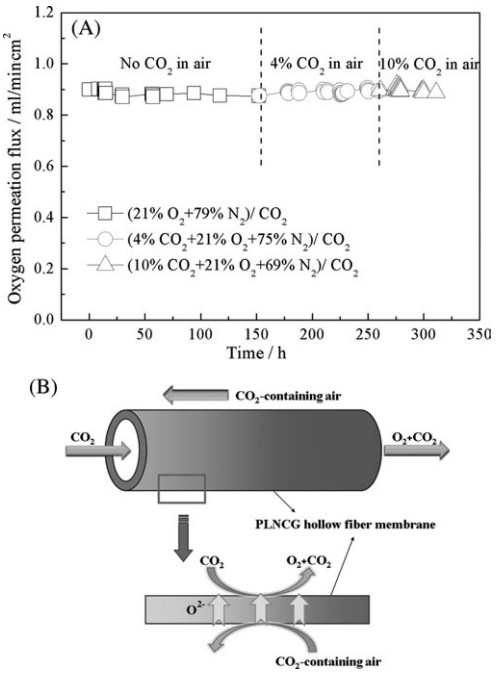

Figure 9. (A) Long-term operation of the oxygen permeation through the U-shaped PLNCG hollow fiber membrane with pure CO_2 as the sweep gas at 975°C. Conditions: $F_{N_2+\ O2+CO2} = 180$ mL/min, $F_{CO_2} = 60$ mL/min, CO_2 concentration in the feed gas kept 0% for 160 h, 4% for 100 h and 10% for 50 h, respectivily, and (B) Model of the oxygen separation through the PLNCG hollow fiber membrane swept by pure CO_2.

hollow fiber membrane. The particles on both the inner and outer surfaces in this K_2NiF_4-type PLNCG system looks like aciculate and it can be noted that the PLNCG particles connect to each other firmly. Figure 11C and D presents the inner and outer surface of the spent PLNCG hollow fiber membrane after 310 h oxygen permeation test using pure CO_2 as the sweep gas and CO_2-containing air as the feed gas (in Figure 9). Although there are some tiny holes on the inner surface of the spent hollow fiber membrane, most part

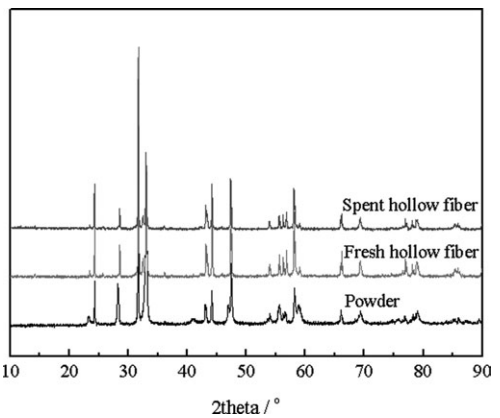

Figure 10. XRD patterns of the PLNCG powder, fresh and spent hollow fiber membrane after 310 h' operation (in Figure 9).

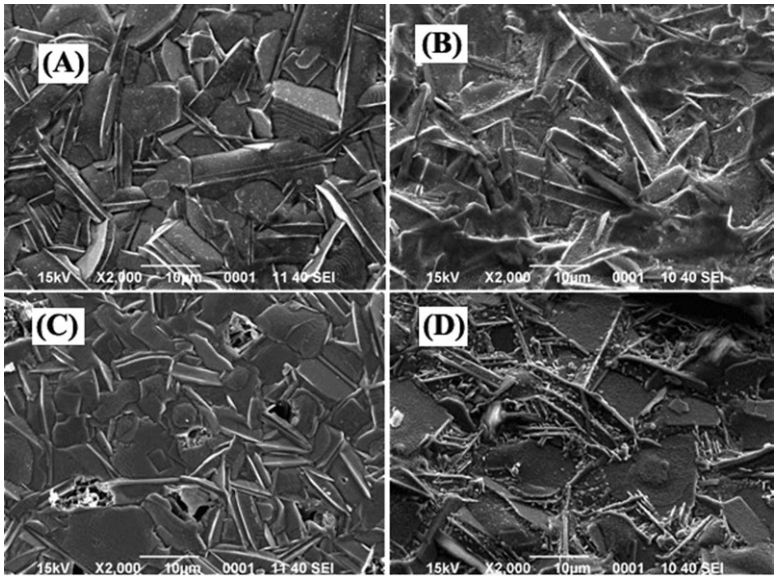

Figure 11. SEM micrographs of the PLNCG hollow fiber membrane.

(A) inner surface, (B) outer surface of the fresh hollow fiber, (C) inner surface, and (D) outer surface of the spent hollow fiber after 310 h' operation (in Figure 9).

of the inner surface keeps intact and no carbon was detected by EDS. The impurity on the outer surface exposed to the air of the spent hollow fiber membrane contains Al and Si, which was detected by EDS. They are from the decomposition of the ceramic sealant. In summary, both of the inner and outer surfaces of the spent PLNCG hollow fiber membrane keeps intact and the PLNCG particles still connect to each other firmly.

Table 2 summarizes the CO_2 effect on the oxygen permeation fluxes through various membranes based on different mixed conducting oxides. As shown in Table 2, when the membrane is exposed to a CO_2-containing atmosphere or even pure CO_2 atomsphere, the decreases of the oxygen permeation fluxes through most of the membranes are more than 90%, such as BSCF. It is because these membranes contain alkaline-earth metals, which tend to react with CO_2. On the other hand, carbonate appears in most phase structures after these membrane exposed to CO_2-containing atmosphere. However, the situation is much better in alkaline-earth metal-free systems, such as $La_{0.85}Ce_{0.1}Ga_{0.3}Fe_{0.65}Al_{0.05}O_{3-\delta}$, $40\%NiFe_2O_4 - 60\%Ce_{0.9}Gd_{0.1}O_{2-\delta}$ and PLNCG listed in Table 2. The decreases of the oxygen permeation fluxes through these membranes are not only less than 40%, the phase structures also keep their's initial structure-types without carbonate. Among these three alkaline-earth metal-free membranes, the PLNCG hollow fiber membrane investigated in present work exhibits excellent performance. The decrease of the oxygen permeation flux through the PLNCG hollow fiber membrane is only 6% at 975°C, which is the least one among all these mixed conducting oxides reported. Furthermore, the operation time of oxygen separation through the U-shaped PLNCG hollow fiber membrane swept by pure CO_2 is more than 310 h, which is the longest one reported and the feed gas also contains CO_2 simultaneously. The constant oxygen permeation flux through the PLNCG membrane in such a rigorous conditions indicates the excellent phase stability of the U-shaped PLNCG hollow fiber membrane.

All these above results demostrate that the U-shaped PLNCG hollow fiber membrane exhibits good oxygen permeability and excellent phase stability under CO_2-containing atomosphere, which indicates its potential applications in the oxyfuel techniques and CO_2 capture process.

Conclusion

The U-shaped K_2NiF_4-type oxide hollow fiber membranes based on $(Pr_{0.9}La_{0.1})_2(Ni_{0.74}Cu_{0.21}Ga_{0.05})O_{4+\delta}$ (PLNCG) are successfully prepared by a phase inversion spinning process. The effects of CO_2 concentration in the sweep gas and the feed gas, as well as the flow rate of pure CO_2 as the sweep gas on the oxygen permeation flux through the PLNCG hollow fiber membrane at different temperatures are investigated in detail. Compared with the oxygen permeation flux under Air/He gradient, the most serious decrease of oxygen

Table 2. Comparison of the CO_2 Effect on the Oxygen Permeation Fluxes Through the Membranes Based on Different Mixed Conducting Oxides

Material	T / °C	Sweep gas	J_{O2} decrease	Phase structure after exposure	Lifetime	Ref.
$La_{0.85}Ce_{0.1}Ga_{0.3}Fe_{0.65}Al_{0.05}O_{3-\delta}$	950	$20\%CO_2+80\%He$	37%	No obvious degradation		40
$BaCo_xFe_yZr_zO_{3-\delta}(x+y+z=1)$	900	$20\%CO_2+80\%He$	93%	$BaCO_3$		29
$BaCo_{0.4}Fe_{0.4}Nb_{0.2}O_{3-\delta}$	900	pure CO_2	93%	$BaCO_3$, CoO		27
$Ba_{0.5}Sr_{0.5}Co_{0.8}Fe_{0.2}O_{3-\delta}$	875	pure CO_2	97%	$(Ba_{0.4}Sr_{0.6})CO_3$, CoO		26
$Ba_{0.5}Sr_{0.5}Fe_{0.8}Zn_{0.2}O_{3-\delta}$	750	pure CO_2	100%	$(Ba_{0.4\pm0.1}Sr_{0.6\pm0.1})CO_3$, ZnO		30
$40\%NiFe_2O_4$ - 60% $Ce_{0.9}Gd_{0.1}O_{2-\delta}$	1000	pure CO_2	10%	No carbonate	>100 h	41
PLNCG	975	pure CO_2	6%	No carbonate	>310 h	This work

permeation flux is only 6% when pure CO_2 is used as the sweep gas on the core side. When the pure CO_2 is used as the sweep gas and even 10% CO_2 was added in the feed air simultaneously, a steady oxygen permeation flux of 0.9 mL/min·cm^2 (STP) is obtained at 975°C and no decline of the oxygen permeation flux is observed. XRD, SEM and EDS characterizations indicate that the spent membrane still maintains the perfect K_2NiF_4-type phase structure and intact microstructure without carbonate. All of these results demonstrate that the U-shaped PLNCG hollow fiber membrane is a promising stable membrane under CO_2-containing atmosphere and has a great potential for the practical application in oxyfuel techniques for CO_2 capture and storage technologies.

Acknowledgments

The authors greatly acknowledge the financial support by Natural Science Foundation of China (nos. 21176087, U0834004, 20936001), the National Basic Research Program of China (no. 2009CB623406), the Science-Technology Plan of Guangzhou City (2009J1-C511-1) and the Fundamental Research Funds for the Central Universities, SCUT (2009220038).

Literature Cited

1. Neftel A, Moor E, Oeschger H, Stauffer B. Evidence from polar ice cores for the increase in atmospheric co$_2$ in the past two centuries. *Nature*. 1985;315:45–47.
2. Tans P. NOAA/ESRL. Trends in Carbon Dioxide. Available at http:// www.esrl.noaa.gov/gmd/ccgg/trends/.
3. Keeling RF, Piper SC, Bollenbacher AF, Walker JS. *2009. Atmospheric CO_2 records from sites in the sio sampling network*. In: *Trends. A Compendium of Data on Global Change*. Carbon Dioxide Information Analyses Center, Oak Ridge National Laboratory, US Dept. of Energy, Oak Ridge, TN;2009. doi:10.3334/CDIAC/atg.035.
4. International Energy Agency. Key World Energy Statistics; 2008. Available at http://www.iea.org/textbase/nppdf/free/2008/key_stats_2008.pdf.
5. Figueroa JD, Fout T, Plasynski S, Mcllvried H, Srivastava RD. Advances in CO_2 capture technology. The US Dept. of Energy's Carbon Sequestration Program. *Int J Greenh Gas Con*. 2008;2:9–20.
6. Gough C. State of the art in carbon dioxide capture and storage in the UK: An experts' review. *Int J Greenh Gas Con*. 2008;2:155–168.
7. Kneer R, Toporov D, Forster M, Christ D, Broeckmann C, Pfaff E, Zwick M, Engels S, Modigell M. OXYCOAL-AC: towards an integrated coal-fired power plant process with ion transport membrane-based oxygen supply. *Energy Environ Sci*. 2010;3:198–207.
8. Ren JY, Fan YQ, Egolfopoulos FN, Tsotsis TT. Membrane-based reactive separations for power generation applications: oxygen lancing. *Chem Eng Sci*. 2003;58:1043–1052.
9. Fan YQ, Ren JY, Onstot W, Pasale J, Tsotsis TT, Egolfopoulos FN. Reactor and technical feasibility aspects of a CO_2 decomposition-based power generation cycle, utilizing a high-temperature membrane reactor. *Ind Eng Chem Res*. 2003;42:2618–2626.
10. Richards GA, Casleton KH, Chorpening BT. CO_2 and H_2O diluted oxy-fuel combustion for zero-emission power. *Proc IMechE Part A*. 2005;219:121–126.
11. Rezvani S, Huang Y, Mcllveen-Wright D, Hewitt N, Mondol JD. Comparative assessment of coal fired IGCC systems with CO_2 capture using physical absorption, membrane reactors and chemical looping. *Fuel*. 2009;88:2463–2472.
12. Buhre BJP, Elliott LK, Sheng CD, Gupta RP, Wall TF. Oxy-fuel combustion technology for coal-fired power generation. *Prog Energy Combust Sci*. 2005;31:283–307.
13. Tan XY, Li K, Thursfield A, Metcalfe IS. Oxyfuel combustion using a catalytic ceramic membrane reactor. *Catal Today*. 2008;131:292–304.
14. Teraoka Y, Zhang HM, Yamazoe N. Oxygen-sorptive properties of defect perovskite-type $La_{1-x}Sr_xCo_{1-y}Fe_yO_{3-\delta}$. *Chem Lett*. 1985;9:1367–1370.
15. Kharton VV, Tikhonovich VN, Li SB, Naumovich EN, Kovalevsky AV, Viskup AP, Bashmakov IA, Yaremchenko AA. Ceramic microstructure and oxygen permeability of $SrCo(Fe,M)O_{3-\delta}$ (M = Cu or Cr) perovskite membranes. *J Electrochem Soc*. 1998;145:1363–1373.
16. Nagai T, Ito W, Sakon T. Relationship between cation substitution and stability of perovskite structure in $SrCoO_{3-\delta}$ -based mixed conductors. *Solid State Ionics*. 2007;177:3433–3444.
17. Qiu L, Lee TH, Liu LM, Yang YL, Jacobson AJ. Oxygen permeation studies of $SrCo_{0.8}Fe_{0.2}O_{3-\delta}$. *Solid State Ionics*. 1995;76:321–329.
18. Elshof ten JE, Bouwmeester HJM, Verweij H. Oxygen-transport through $La_{1-x}Sr_xFeO_{3-\delta}$ membranes. 1. Permeation in air/He gradients. *Solid State Ionics*. 1995;81:97–109.
19. Tsai CY, Dixon AG, Ma YH, Moser WR, Pascucci MR. Dense perovskite, $La_{(1-x)}A'_xFe_{1-y}Co_yO_{3-\delta}$ (A' = Ba, Sr, Ca), membrane synthesis, applications and characterization. *J Am Ceram Soc*. 1998;81:1437–1444.
20. Teraoka Y, Zhang HM, Furukawa S, Yamazoe N. Oxygen permeation through perovksite-type oxides. *Chem Lett*. 1985;11:1743–1748.
21. Shao ZP, Yang WS, Cong Y, Dong H, Tong JH, Xiong GX. Investigation of the permeation behavior and stability of a $Ba_{0.5}Sr_{0.5}Co_{0.8}Fe_{0.2}O_{3-\delta}$ oxygen membrane. *J Membr Sci*. 2000;172:177–188.
22. Li QM, Zhu XF, Yang WS. Investigation of structure and oxygen permeability of Ba-Ce-Co-Fe-O system. *Mater Res Bull*. 2010;45:1112–1117.
23. Yin QH, Lin YS. Effect of dopant addition on oxygen sorption properties of La-Sr-Co-Fe-O perovskite type oxide. *Adsorption*. 2006;12:329–338.
24. Yin QH, Yang ZH, Lin YS. Effects of microstructure on oxygen transport in perovskite-type oxides. *J Mater Sci*. 2006;41:4865–4870.
25. Qi XW, Lin YS, Holt CT, Swartz SL. Electric conductivity and oxygen permeability of modified cerium oxides. *J Mater Sci*. 2003;38:1073–1079.
26. Arnold M, Wang HH, Feldhoff A. Influence of CO_2 on the oxygen permeation performance and the microstructure of perovskite-type $(Ba_{0.5}Sr_{0.5})(Co_{0.8}Fe_{0.2})O_{3-\delta}$ membranes. *J Membr Sci*. 2007;293:44–52.
27. Yi JX, Schroeder M, Weirich T, Mayer J. Behavior of Ba(Co, Fe, Nb)$O_{3-\delta}$ perovskite in CO_2-containing atmospheres: degradation mechanism and materials design. *Chem Mater*. 2010;22:6246–6253.
28. Yang Z, Harvey AS, Gauckler LJ. Influence of CO_2 on $Ba_{0.2}Sr_{0.8-}Co_{0.8}Fe_{0.2}O_{3-\delta}$ at elevated temperatures. *Script Mater*. 2009;61:1083–1086.
29. Czuprata O, Arnold M, Schirrmeister S, Schiestel T, Caro J. Influence of CO_2 on the oxygen permeation performance of perovskite-type $BaCo_xFe_yZr_zO_{3-\delta}$hollow fiber membranes. *J Membr Sci*. 2010;364:132–137.
30. Martynczuk J, Efimov K, Robben L, Feldhoff A. Performance of zinc-doped perovskite-type membranes at intermediate temperatures for long-term oxygen permeation and under a carbon dioxide atmosphere. *J Membr Sci*. 2009;344:62–70.
31. Yang Q, Lin YS, Bulow M. High temperature sorption separation of air for producing oxygen-enriched CO_2 stream. *AIChE J*. 2006;52:574–581.
32. Tong JH, Yang WS, Zhu BC, Cai R. Investigation of ideal zirconium-doped perovskite-type ceramic membrane materials for oxygen separation. *J Membr Sci*. 2002;203:175–189.
33. Yi JX, Feng SJ, Zuo YB, Liu W, Chen CS. Oxygen permeability and stability of $Sr_{0.95}Co_{0.8}Fe_{0.2}O_{3-\delta}$ in a CO_2- and H_2O-containing atmosphere. *Chem Mater*. 2005;17:5856–5861.
34. Park JH, Kim JP, Son SH. Oxygen permeation and stability of $Ba_{0.5}Sr_{0.5}Co_{0.8}Fe_{0.2}O_{3-\delta}$ membrane according to trace elements and oxygen partial pressure in synthetic air. *Energy Procedia*. 2009;1:369–374.
35. Jin WQ, Zhang C, Zhang P, Fan YQ, Xu NP. Thermal decomposition of carbon dioxide coupled with POM in a membrane reactor. *AIChE J*. 2006;52:2545–2550.
36. Jin WQ, Zhang C, Chang XF, Fan YQ, Xing WH, Xu NP. Efficient catalytic decomposition of CO_2 to CO and O_2 over Pd/mixed-conducting oxide catalyst in an oxygen-permeable membrane reactor. *Environ Sci Technol*. 2008;42:3064–3068.
37. Zuo CD, Dorris SE, Balachandran U, Liu ML. Effect of Zr-doping on the chemical stability and hydrogen permeation of the Ni-$BaCe_{0.8}Y_{0.2}O_{3-\delta}$ mixed protonic-electronic conductor. *Chem Mater*. 2006;18:4647–4650.
38. Zeng Q, Zuo YB, Fan CG, Chen CS. CO_2-tolerant oxygen separation membranes targeting CO_2 capture application. *J Membr Sci*. 2009;335:140–144.
39. Carolan MF, Motika SA, Dyer PN, Alba PB. Novel compositions capable of operating under high carbon dioxide partial pressures for use in solid-state oxygen producing devices. EP Patent 0732306. 1996.

40. Dong XL, Zhang GR, Liu ZK, Zhong ZX, Jin WQ, Xu NP. CO_2-tolerant mixed conducting oxide for catalytic membrane reactor. *J Membr Sci*. 2009;340:141–147.
41. Luo HX, Efimov K, Jiang HQ, Feldhoff A, Wang HH, Caro J. CO_2-stable and cobalt-free dual-phase membrane for oxygen separation. *Angew Chem Int Ed*. 2011;50:759–763.
42. Caro J, Wang HH, Tablet C, Kleinert A, Feldhoff A, Schiestel T, Kilgus M, Kolsch P, Werth S. Evaluation of perovskites in hollow fibre and disk geometry in catalytic membrane reactors and in oxygen separators. *Catal Today*. 2006;118:128–135.
43. Li C, Yu GY, Yang NR. Supported dense oxygen permeating membrane of mixed conductor $La_2Ni_{0.8}Fe_{0.2}O_{4+\delta}$ prepared by sol-gel method. *Sep Purif Technol*. 2003;32:335–339.
44. Yashima M, Sirikanda N, Ishihara T. Crystal structure, diffusion path, and oxygen permeability of a Pr_2NiO_4-Based mixed conductor $(Pr_{0.9}La_{0.1})_2(Ni_{0.74}Cu_{0.21}Ga_{0.05})O_{4+\delta}$. *J Am Chem Soc*. 2010;132:2385–2392.
45. Liu SM, Gavalas GR. Preparation of oxygen ion conducting ceramic hollow-fiber membranes. *Ind Eng Chem Res*. 2005;44:7633–7637.
46. Tan XY, Liu Y, Li K. Mixed conducting ceramic hollow-fiber membranes for air separation. *AIChE J*. 2005;51:1991–2000.
47. Tan XY, Li K. Oxygen production using dense ceramic hollow fiber membrane modules with different operating modes. *AIChE J*. 2007;53:838–845.
48. Liu SM, Tan XY, Li K, Hughes R. Preparation and characterisation of $SrCe_{0.95}Yb_{0.05}O_{2.975}$ hollow fiber membranes. *J Membr. Sci*. 2001;193:249–260.
49. Liu SM, Tan XY, Shao ZP, da Costa JCD. $Ba_{0.5}Sr_{0.5}Co_{0.8}Fe_{0.2}O_{3-\delta}$. ceramic hollow-fiber membranes for oxygen permeation. *AIChE J*. 2006;52:3452–3461.
50. Schiestel T, Kilgus M, Peter S, Caspary KJ, Wang HH, Caro J. Hollow fibre perovskite membranes for oxygen separation. *J Membr Sci*. 2005:258:1–4.
51. Trunec M. Fabrication of zirconia- and ceria-based thin-wall tubes by thermoplastic extrusion. *J Euro Ceram Soc*. 2004;24:645–651.
52. Luyten J, Buekenhoudt A, Adriansens W, Cooymans J, Weyten H, Servaes F, Leysen R. Preparation of $LaSrCoFeO_{3-\delta}$ membranes. *Solid State Ionics*. 2000;135:637–642.
53. Wei YY, Liu HF, Xue J, Li Z, Wang HH. Preparation and oxygen permeation of U-shaped perovskite hollow fiber membranes. *AIChE J*. 2011;57:975–984.

Manuscript received July 21, 2011, and revision received Oct. 8, 2011.